Higher fully-charmed tetraquarks: radial excitations and P-wave states

Guang-Juan Wang

Japan Atomic Energy Agency

In collaboration with L. Meng, M. Oka and S. L. Zhu

Base on: Phys. Rev. D. 100, 096013 (2019) and arXiv: 2105.13109.

Background

- Since the discovery of X(3872) in 2003, numerous exotic structures "XYZ" and pentaquark states have been observed in experiments.

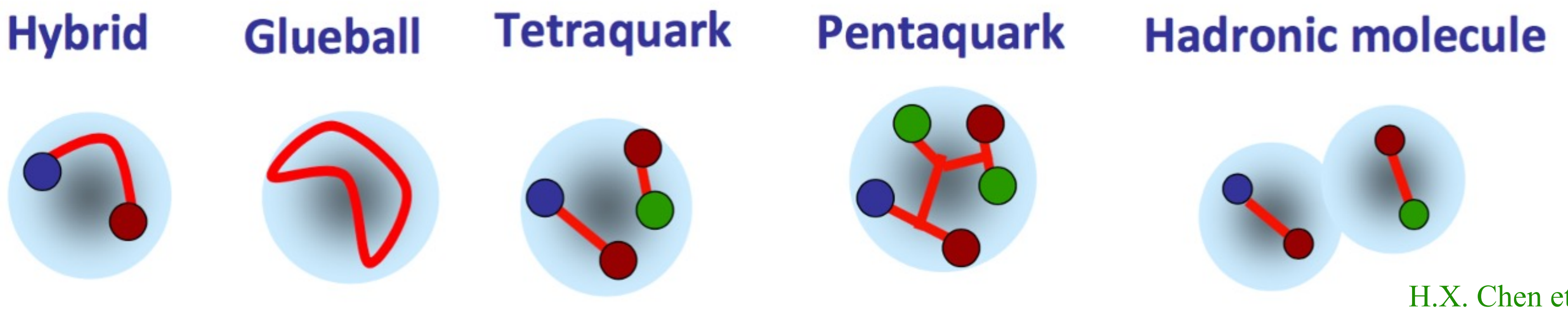

H.X. Chen et al., Phys. Rept. 639, 1
F. K. Guo et al., Rev. Mod. Phys., 015004
Y. R. Liu et al., Prog.Part.Nucl.Phys. 107 237-320
C. Z. Yuan, Int.J.Mod.Phys. A33,1830018

- Light quark q ($q = u, d, s$) makes problem complicated

✓ Loosely bound molecule VS. compact tetraquarks.

✓ Coupled-channel effect: $\bar{\text{Q}}$Q meson core & Q$\bar{\text{Q}}q\bar{\text{q}}$.

✓ Relativistic effects.

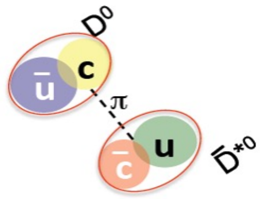

molecule

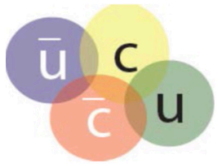

tetraquark

Fully-heavy tetraquark

• The fully-heavy tetraquark state $T_{Q_1 Q_2 \bar{Q}_3 \bar{Q}_4} (Q = c, b)$ is a good candidate for compact tetraquark state.

✓ Heavy quarks: short range one-gluon-exchange (OGE) potential dominates.

✓ The light-meson-exchange interaction is suppressed (unlikely molecule).

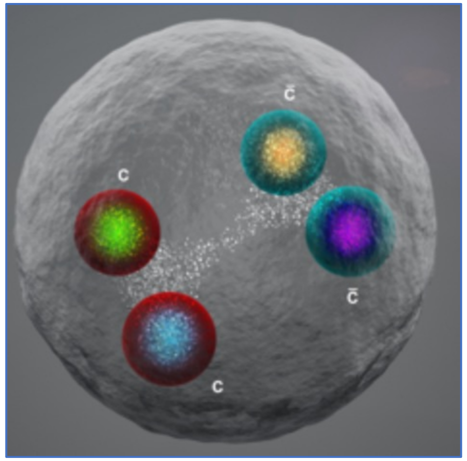

• Diquark-antidiquark (QQ)-$(\bar{Q}\bar{Q})$: $\bar{3}_c \otimes 3_c = 1_c$ and $6_c \otimes \bar{6}_c = 1_c$.

• Golden platform to investigate multi-quark system.

Experimental search for $T_{bb\bar{b}\bar{b}}$

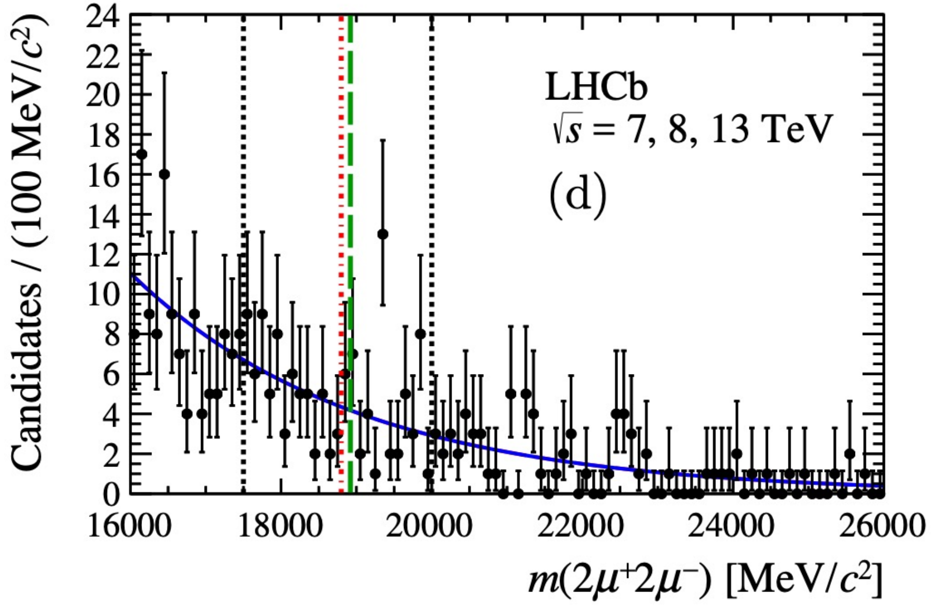

JHEP 1810, 086 (2018).

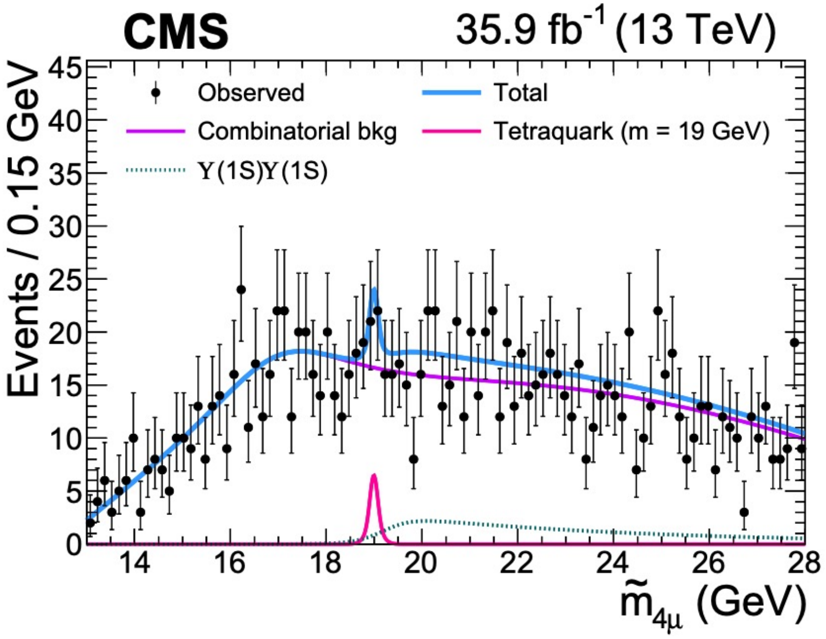

arXiv: 2002.06393

- LHCb and CMS: search for $T_{bb\bar{b}\bar{b}}$ in $\Upsilon(1S)\mu^+\mu^-$ invariant mass spectrum.
- No significant excess observed for $T_{bb\bar{b}\bar{b}}$.
- CMS: An example signal at 19 GeV with a significance of about one standard deviation.

Experimental search for $T_{cc\bar{c}\bar{c}}$

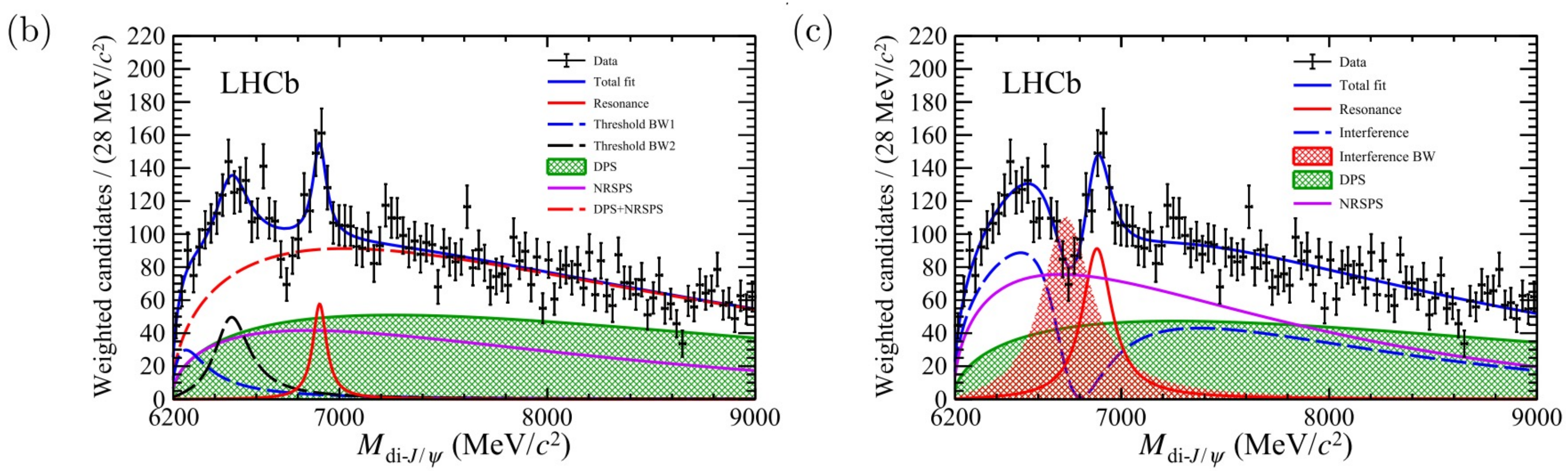

Science Bulletin 65 (2020) 1983.

- Search for $T_{cc\bar{c}\bar{c}}$ in di-J/ψ channel.
- A broad structure ranging $(6.2, 6.8)$ GeV.
- $X(6900)$: A narrow peaking structure at 6.9 GeV with the signal significance > 5σ.
- The theoretical prediction for ground S-wave $T_{cc\bar{c}\bar{c}}$: $(6.3, 6.5)$ GeV.
- $X(6900)$ is an candidate for excited tetraquark state.

Formalism

- The strong interactions : one-gluon exchange (OGE) plus phenomenological linear confinement.

Phys. Rev. D 72, 054026

$$H = H_0 + \frac{\lambda_i}{2} \cdot \frac{\lambda_j}{2} [V_{\text{cen}}^{(0)}(r_{ij}) + V_{\text{so}}^{(1)}(r_{ij}) + V_{\text{tens}}^{(1)}(r_{ij})]$$

$$H_0 = \sum_{i=1}^{4} \frac{\mathbf{p}_i^2}{2m_i} + \sum_i m_i - T_G.$$

$$V_{\text{cen}}^{(0)}(r_{ij}) = \frac{\alpha_s}{r_{ij}} - \frac{3}{4} b r_{ij} - \frac{8\pi\alpha_s}{3m_i m_j} \left(\frac{\sigma}{\sqrt{\pi}}\right)^3 e^{-\sigma^2 r_{ij}^2} \mathbf{s}_i \cdot \mathbf{s}_j.$$

- $V_{cen}^{(0)}$: OGE Coulomb + linear confinement + hyperfine

Phys. Rev. D 32, 189

- $V_{so}^{(1)} + V_{tens}^{(1)}$: spin-orbital and tensor interactions & perturbatively.

$$V_{\text{so}}^{(1)}(r_{ij}) = V_{\text{so}}^{v}(r_{ij}) + V_{\text{so}}^{s}(r_{ij}).$$

$$V_{\text{so}}^{v}(r_{ij}) = \frac{1}{r_{ij}} \frac{dV_{\text{Coul}}}{dr_{ij}} \frac{1}{4} \Big[\left(\frac{1}{m_i^2} + \frac{1}{m_j^2} + \frac{4}{m_i m_j} \right) \mathbf{L}_{ij} \cdot \mathbf{S}_{ij} + \left(\frac{1}{m_i^2} - \frac{1}{m_j^2} \right) \mathbf{L}_{ij} \cdot (\mathbf{s}_i - \mathbf{s}_j) \Big]$$

$$V_{\text{so}}^{s}(r_{ij}) = -\frac{1}{r_{ij}} \frac{dV_{\text{lin}}}{dr_{ij}} \left(\frac{\mathbf{L}_{ij} \cdot \mathbf{s}_i}{2m_i^2} + \frac{\mathbf{L}_{ij} \cdot \mathbf{s}_j}{2m_j^2} \right)$$

$$V_{\text{tens}}^{(1)}(r_{ij}) = -\left(\frac{\partial^2}{\partial r_{ij}^2} - \frac{1}{r_{ij}} \frac{\partial}{\partial r_{ij}} \right) \frac{V_{\text{Coul}}}{3m_i m_j} \mathcal{S}_{ij}$$

Formalism

TABLE I. The parameters of the quark model and the corresponding mass spectrum (THE) of the charmonia $c\bar{c}$ compared with their experimental values (EXP) [89]. PDG 2020

parameter		Mass spectrum (MeV)			
		$^{2S+1}L_J$	Meson	EXP	THE
α_s	0.5461	$^1S_0$	η_c	2983.9	2984
b [GeV^2]	0.1452	$^3S_1$	J/ψ	3096.9	3092
m_c [GeV]	1.4794	$^3P_0$	χ_{c0}	3414.7	3426
σ [GeV]	1.0946	$^3P_1$	χ_{c1}	3510.7	3506
		$^1P_1$	$h_c(1P)$	3525.4	3516
		$^3P_2$	χ_{c2}	3556.2	3556
		$^1S_0$	$\eta_c(2S)$	3637.5	3634
		$^3S_1$	$\psi(2S)$	3686.1	3675
		$^3S_1$	$\psi(3S)$	4039.0	4076
		$^3S_1$	$\psi(4S)$	4421.0	4412

- Four parameters are determined by mass spectra of $c\bar{c}$.
- Calculate the mass spectrum in two stages.

✓ $H = H_0 + V_{cen}^{(0)}$ (OGE Coulomb+ confinement+ hyperfine) & Schrödinger equation to obtain $\psi_{JJ_z}^0$.

✓ $V = V_{cen}^{(0)} + V_{so}^{(1)} + V_{tens}^{(1)}$ & diagonalizing the Hamiltonian matrix in the basis of $\psi_{JJ_z}^0$.

✓ Extended to study $T_{cc\bar{c}\bar{c}}$.

Formalism

- Few-body problem: Gaussian expansion method Prog. Part. Nucl. Phys. 51 223-307

$$\psi_{JJ_z} = \sum \left[\varphi_{n_a J_a}(\mathbf{r}_{12}, \beta_a) \otimes \varphi_{n_b J_b}(\mathbf{r}_{34}, \beta_b) \otimes \phi_{N L_{ab}}(\mathbf{r}, \beta)\right]_{JJ_z} ,$$

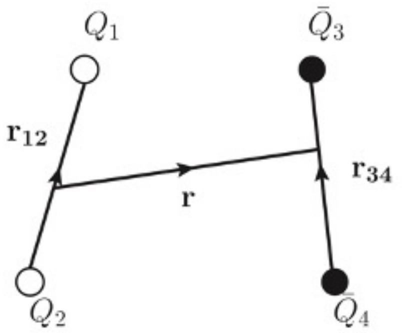

- Basic wave function of each Jacobi coordinate

$$\varphi_{n_a J_a M_a} = [\phi_{n_a l_a}(\mathbf{r}_{12}, \beta_a)\chi_{s_a}]^{J_a}_{M_a} \chi_f \chi_{c_a}$$

- Gaussian function:

$$\phi_{n_a l_a}(r_{12}, \beta_a) = \left\{\frac{2^{l_a+2}(2\nu_{n_a})^{l+3/2}}{\sqrt{\pi}(2l_a+1)!!}\right\}^{1/2} r_{12}^{l_a} e^{-\nu_{n_a} r_{12}^2}$$

- Construct the color-spin-flavor configurations with diquark and antidiquark.

TABLE II. The color-flavor-spin configurations of the QQ ($\bar{Q}\bar{Q}$) diquark (antidiquark).

Flavor	S-wave($L=0$)	Spin	Color		J^P
S	S	S($S_{QQ}=1$)	$\bar{3}_c$(A)	$[QQ]^1_{\bar{3}_c}$	1^+
S	S	A($S_{QQ}=0$)	6_c(S)	$[QQ]^0_{6_c}$	0^+
Flavor	**P-wave ($L=1$)**	**Spin**	**Color**		
S	A	S($S_{QQ}=1$)	6_c(S)	$[[QQ]^1_{6_c}, \rho]^0_{6_c}$	0^-
				$[[QQ]^1_{6_c}, \rho]^1_{6_c}$	1^-
				$[[QQ]^1_{6_c}, \rho]^2_{6_c}$	2^-
S	A	A($S_{QQ}=0$)	$\bar{3}_c$(A)	$[[QQ]^0_{\bar{3}_c}, \rho]^1_{\bar{3}_c}$	1^-

S-wave $T_{cc\bar{c}\bar{c}}$

- The S-wave $T_{cc\bar{c}\bar{c}}$ state: $L_{12} = L_{34} = L_r = 0$.
- $V_{so}^{(1)} + V_{tens}^{(1)}$: couple with non-S wave excited state & neglected.
- Color-flavor-spin wavefunction:

$$0^{++} \quad [[QQ]^1_{\bar{3}_c}[\bar{Q}\bar{Q}]^1_{3_c}]^0_{1_c} \quad [[QQ]^0_{6_c}[\bar{Q}\bar{Q}]^0_{\bar{6}_c}]^0_{1_c}$$

$$1^{+-} \quad [[QQ]^1_{\bar{3}_c}[\bar{Q}\bar{Q}]^1_{3_c}]^1_{1_c}$$

$$2^{++} \quad [[QQ]^1_{\bar{3}_c}[\bar{Q}\bar{Q}]^1_{3_c}]^2_{1_c}$$

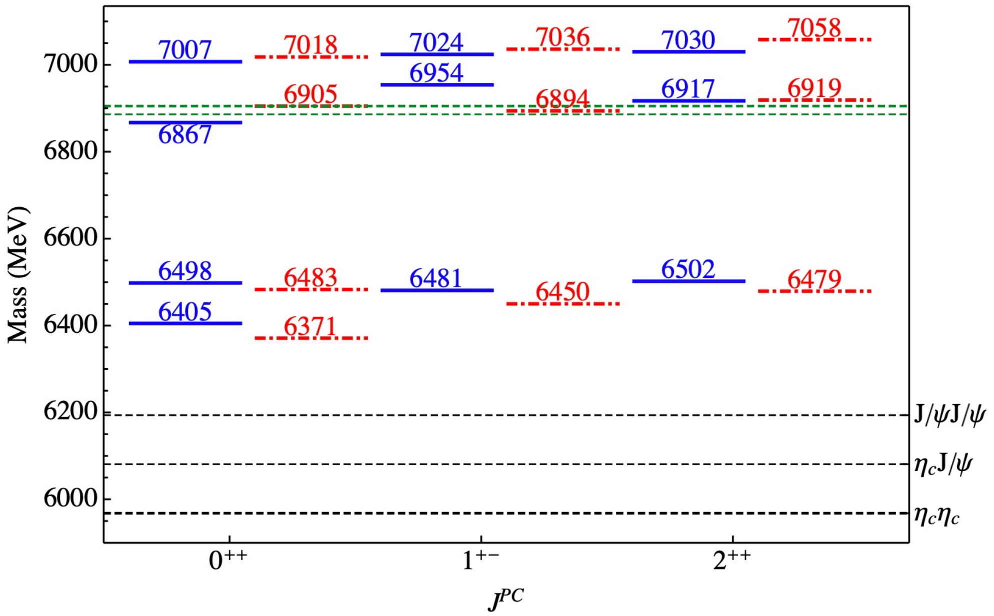

FIG. 2. The mass spectrum of the S-wave tetraquark states T_c. The dot-dashed red and the blue bars represent the mass spectra from two quark models and. The green dashed lines stand for the $X(6900)$ mass in the two fits obtained by experiments.

- 0^{++} state: an admixture of $\bar{3}_c - 3_c$ and $6_c - \bar{6}_c$ configurations.
- No bound states exist in the quark model.
- Wide S-wave $T_{cc\bar{c}\bar{c}}$: di- J/ψ, di- η_c, $\eta_c J/\psi$.
- $X(6900)$: wide S-wave states $J^{PC} = 0^{++}$ or 2^{++}.

J^{PC}	Decay Modes
0^{++}	$\eta_c\eta_c$, $\boldsymbol{J/\psi J/\psi}$, $\chi_{c1}\eta_c$(P-wave), $J/\psi h_c(1P)$(P-wave), $J/\psi\psi(2S)$, $\chi_{c0}\chi_{c0}$
1^{+-}	$\eta_c J/\psi$, $h_c\eta_c$(P-wave), $J/\psi\chi_{c1}$(P-wave), $\eta_c\psi'$, $h_c\chi_{c0}$
2^{++}	$\boldsymbol{J/\psi J/\psi}$, $\eta_c\chi_{c1}$(P-wave), $\eta_c\chi_{c2}$(P-wave), $J/\psi h_c$(P-wave), $J/\psi\psi(2S)$, $\chi_{c0}\chi_{c2}$

S-wave $T_{cc\bar{c}\bar{c}}$

- $J^{PC} = 0^{++}$:

0^{++}	Mass	$\bar{3}_c \otimes 3_c$	$6_c \otimes \bar{6}_c$	$1_c \otimes 1_c$	$8_c \otimes 8_c$	r_{12}/r_{34}	r	r_{13}/r_{24}	r'
1S	6405	31.9%	68.1%	96.9%	3.13%	0.52	0.31	0.48	0.37
	6498	67.7%	32.3%	5.7%	94.3%	0.51	0.36	0.51	0.36
2S	6867	10.6%	89.4%	80.6%	19.4%	0.65	0.35	0.58	0.46
	7007	89.7%	10.3%	26.0%	74.0%	0.49	0.47	0.59	0.35

- 0^{++} ground state: $6_c - \bar{6}_c$ component is lighter and dominates.
- The root mean square is small.

$-\frac{1}{3}$, attractive

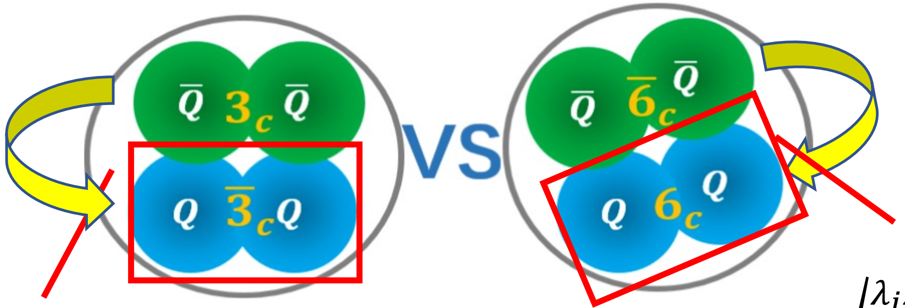

$-\frac{5}{6}$, attractive

Compete

$\left\langle \frac{\lambda_i \lambda_j}{2} \right\rangle = -\frac{2}{3}$, attractive

$\left\langle \frac{\lambda_i \lambda_j}{2} \right\rangle = \frac{1}{3}$, repulsive

P-wave $T_{cc\bar{c}\bar{c}}$

- P-wave state: λ-and ρ- mode excitations.
- Color-flavor-spin wavefunction: same except coupling of the spin and orbital angular momentum.
- $H = H_0 + V_{cen}^{(0)}$ in Schrödinger equation.
- $V_{so}^{(1)} + V_{tens}^{(1)}$ contribute to mass shifts.

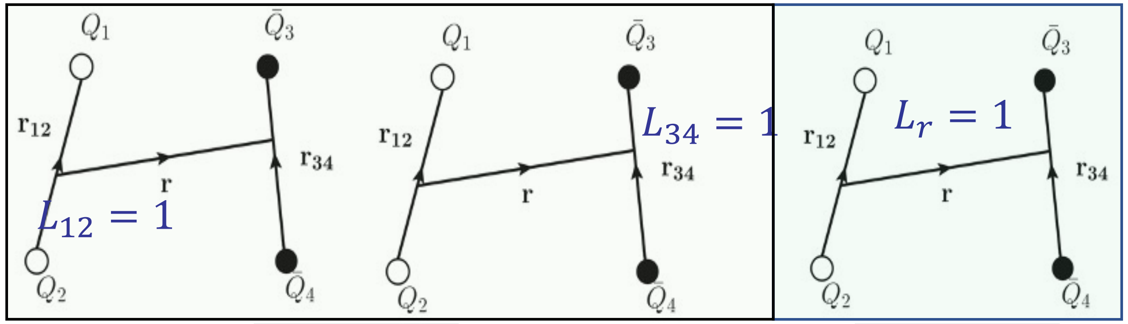

ρ-mode **λ-mode**

		λ-mode	ρ-mode
	0^{-+}	$\vert 3_\lambda^+;{}^3P_0\rangle = \left[\left[[QQ]^1_{\bar{3}_c}[\bar{Q}\bar{Q}]^1_{3_c}\right]^1_{1_c},\lambda\right]^0_{1_c}$	$\vert 3_\rho^+;{}^3P_0\rangle = \frac{1}{\sqrt{2}}\left(\left[\left[[QQ]^0_{\bar{3}_c},\rho\right]^1_{\bar{3}_c}[\bar{Q}\bar{Q}]^1_{3_c}\right]^0 + c.c.\right)$ $\vert 6_\rho^+;{}^3P_0\rangle = \frac{1}{\sqrt{2}}\left(\left[\left[[QQ]^1_{6_c},\rho\right]^0_{6_c}[\bar{Q}\bar{Q}]^0_{\bar{6}_c}\right]^0 + c.c.\right)$
	1^{-+}	$\vert 3_\lambda^+;{}^3P_1\rangle = \left[\left[[QQ]^1_{\bar{3}_c}[\bar{Q}\bar{Q}]^1_{3_c}\right]^1_{1_c},\lambda\right]^1_{1_c}$	$\vert 3_\rho^+;{}^3P_1\rangle = \frac{1}{\sqrt{2}}\left(\left[\left[[QQ]^0_{\bar{3}_c},\rho\right]^1_{\bar{3}_c}[\bar{Q}\bar{Q}]^1_{3_c}\right]^1 + c.c.\right)$ $\vert 6_\rho^+;{}^3P_1\rangle = \frac{1}{\sqrt{2}}\left(\left[\left[[QQ]^1_{6_c},\rho\right]^1_{6_c}[\bar{Q}\bar{Q}]^0_{\bar{6}_c}\right]^1 + c.c.\right)$
	2^{-+}	$\vert 3_\lambda^+;{}^3P_2\rangle = \left[\left[[QQ]^1_{\bar{3}_c}[\bar{Q}\bar{Q}]^1_{3_c}\right]^1_{1_c},\lambda\right]^2_{1_c}$	$\vert 3_\rho^+;{}^3P_2\rangle = \frac{1}{\sqrt{2}}\left(\left[\left[[QQ]^0_{\bar{3}_c},\rho\right]^1_{\bar{3}_c}[\bar{Q}\bar{Q}]^1_{3_c}\right]^2 + c.c.\right)$ $\vert 6_\rho^+;{}^3P_2\rangle = \frac{1}{\sqrt{2}}\left(\left[\left[[QQ]^1_{6_c},\rho\right]^2_{6_c}[\bar{Q}\bar{Q}]^0_{\bar{6}_c}\right]^2 + c.c.\right)$
P-wave	0^{--}	–	$\vert 3_\rho^-;{}^3P_0\rangle = \frac{1}{\sqrt{2}}\left(\left[\left[[QQ]^0_{\bar{3}_c},\rho\right]^1_{\bar{3}_c}[\bar{Q}\bar{Q}]^1_{3_c}\right]^0 - c.c.\right)$ $\vert 6_\rho^-;{}^3P_0\rangle = \frac{1}{\sqrt{2}}\left(\left[\left[[QQ]^1_{6_c},\rho\right]^0_{6_c}[\bar{Q}\bar{Q}]^0_{\bar{6}_c}\right]^0 - c.c.\right)$
	1^{--}	$\vert 3_\lambda^-;{}^1P_1\rangle = \left[\left[[QQ]^1_{\bar{3}_c}[\bar{Q}\bar{Q}]^1_{3_c}\right]^0_{1_c},\lambda\right]^1_{1_c}$ $\vert 6_\lambda^-;{}^1P_1\rangle = \left[\left[[QQ]^0_{6_c}[\bar{Q}\bar{Q}]^0_{\bar{6}_c}\right]^0_{1_c},\lambda\right]^1_{1_c}$ $\vert 3_\lambda^-;{}^5P_1\rangle = \left[\left[[QQ]^1_{\bar{3}_c}[\bar{Q}\bar{Q}]^1_{3_c}\right]^2_{1_c},\lambda\right]^1_{1_c}$	$\vert 3_\rho^-;{}^3P_1\rangle = \frac{1}{\sqrt{2}}\left(\left[\left[[QQ]^0_{\bar{3}_c},\rho\right]^1_{\bar{3}_c}[\bar{Q}\bar{Q}]^1_{3_c}\right]^1 - c.c.\right)$ $\vert 6_\rho^-;{}^3P_1\rangle = \frac{1}{\sqrt{2}}\left(\left[\left[[QQ]^1_{6_c},\rho\right]^1_{6_c}[\bar{Q}\bar{Q}]^0_{\bar{6}_c}\right]^1 - c.c.\right)$
	2^{--}	$\vert 3_\lambda^-;{}^5P_2\rangle = \left[\left[[QQ]^1_{\bar{3}_c}[\bar{Q}\bar{Q}]^1_{3_c}\right]^2_{1_c},\lambda\right]^2_{1_c}$	$\vert 3_\rho^-;{}^3P_2\rangle = \frac{1}{\sqrt{2}}\left(\left[\left[[QQ]^0_{\bar{3}_c},\rho\right]^1_{\bar{3}_c}[\bar{Q}\bar{Q}]^1_{3_c}\right]^2 - c.c.\right)$ $\vert 6_\rho^-;{}^3P_2\rangle = \frac{1}{\sqrt{2}}\left(\left[\left[[QQ]^1_{6_c},\rho\right]^2_{6_c}[\bar{Q}\bar{Q}]^0_{\bar{6}_c}\right]^2 - c.c.\right)$
	3^{--}	$\vert 3_\lambda^-;{}^5P_3\rangle = \left[\left[[QQ]^1_{\bar{3}_c}[\bar{Q}\bar{Q}]^1_{3_c}\right]^2_{1_c},\lambda\right]^3_{1_c}$	

P-wave $T_{cc\bar{c}\bar{c}}$

- $H = H_0 + V_{cen}^{(0)}$:

J^{-+}	Mass	$\vert 3_\lambda^+;^3P_{0,1,2}\rangle$	$\vert 3_\rho^+;^3P_{0,1,2}\rangle$	$\vert 6_\rho^+;^3P_{0,1,2}\rangle$	$1_c\otimes 1_c$	$8_c\otimes 8_c$	
$\vert\lambda_1^+\rangle$	6746	99.5%	0.4%	0.1%	33.4%	66.6%	
J^{-+}	Mass	$\vert 3_\lambda^+;^3P_{0,1,2}\rangle$	$\vert 3_\rho^+;^3P_{0,1,2}\rangle$	$\vert 6_\rho^+;^3P_{0,1,2}\rangle$	$1_c\otimes 1_c$	$8_c\otimes 8_c$	$6_\rho^+ < 3_\lambda^+ < 3_\rho^+$
$\vert\rho_1^+\rangle$	6599	0.1%	24.5%	75.4%	58.5%	41.5%	
$\vert\rho_2^+\rangle$	6894	0.5%	72.0%	27.5%	42.5%	57.5%	
J^{--}	Mass	$\vert 3_\lambda^-;^1P_1\rangle$	$\vert 6_\lambda^-;^1P_1\rangle$	$\vert 3_\lambda^-;^5P_{1,2,3}\rangle$	$1_c\otimes 1_c$	$8_c\otimes 8_c$	
$\vert\lambda_1^-\rangle$	6740	98.9%	1.1%	0%	33.7%	66.3%	
$\vert\lambda_2^-\rangle$	6741	0%	0%	100%	33.3%	66.7%	
$\vert\lambda_3^-\rangle$	6885	1.4%	98.6%	0%	66.2%	33.8%	$6_\rho^- < 3_\lambda^- < 6_\lambda^- < 3_\rho^-$
J^{--}	Mass	$\vert 3_\rho^-;^3P_{0,1,2}\rangle$	$\vert 6_\rho^-;^3P_{0,1,2}\rangle$		$1_c\otimes 1_c$	$8_c\otimes 8_c$	
$\vert\rho_1^-\rangle$	6561	27.1%	72.9%		57.6%	42.4%	
$\vert\rho_2^-\rangle$	6913	72.1%	27.9%		42.6%	57.4%	

- $J^{--/+}(J = 0,1,2,3)$: Same mass spectrum and differences will be induced by $V_{so}^{(1)} + V_{tens}^{(1)}$.
- OGE Coulomb & Linear confinement: do not contribute to the mixing of the λ-and ρ- mode excitations.
- Hyperfine: quite small mixing of λ- and ρ- mode excitation.
- Eigenstates is dominated by one excitation mode.
- $6_\rho < 3_\lambda < 6_\lambda < 3_\rho$.

P-wave $T_{cc\bar{c}\bar{c}}$

- With $V_{so}^{(1)} + V_{tens}^{(1)}$

J^{PC}		Mass	$\|\lambda_1^{+/-}\rangle$	$\|\lambda_2^{-}\rangle$	$\|\lambda_3^{-}\rangle$	$\|\rho_1^{+/-}\rangle$	$\|\rho_2^{+/-}\rangle$	r_{12}/r_{34}	r	r_{13}/r_{24}	r'
1^{--}	$\begin{pmatrix} 6740 & -2 & 0 & -10 & 9 \\ -2 & 6741-23 & 7 & -19 & 26 \\ 0 & 7 & 6885 & -2 & -25 \\ -10 & -19 & -2 & 6561-1 & 21 \\ 9 & 26 & -25 & 21 & 6913-28 \end{pmatrix}$	6555	0.3%	1.6%	$\sim 0\%$	97.5%	0.6%	0.61	0.32	0.59	0.49
		6716	0.6%	94.8%	0.4%	2.0%	2.1%	0.52	0.42	0.65	0.37
		6740	98.8%	0.9%	$\sim 0\%$	0.2%	0.1%	0.51	0.43	0.65	0.36
		6864	0.2%	2.2%	55.7%	0.1%	41.9%	0.62	0.35	0.64	0.47
		6911	0.1%	0.5%	43.9%	0.2%	55.3%	0.61	0.36	0.63	0.47
2^{-+}	$\begin{pmatrix} 6746+6 & 7 & 10 \\ 7 & 6599-6 & 13 \\ 10 & 13 & 6894+18 \end{pmatrix}$	6592	0.2%			99.7%	0.1%	0.63	0.33	0.60	0.50
		6752	99.4%			0.2%	0.4%	0.52	0.43	0.66	0.36
		6913	0.4%			0.2%	99.4%	0.57	0.38	0.60	0.47
2^{--}	$\begin{pmatrix} 6741-2 & 7 & -9 \\ 7 & 6561-6 & -15 \\ -9 & -15 & 6913+20 \end{pmatrix}$	6554		0.1%		99.7%	0.2%	0.61	0.32	0.59	0.49
		6739		99.6%		0.1%	0.2%	0.51	0.43	0.66	0.36
		6934		0.2%		0.2%	99.6%	0.57	0.38	0.61	0.48
3^{--}	$6741+11$	6753		100%				0.51	0.43	0.66	0.36

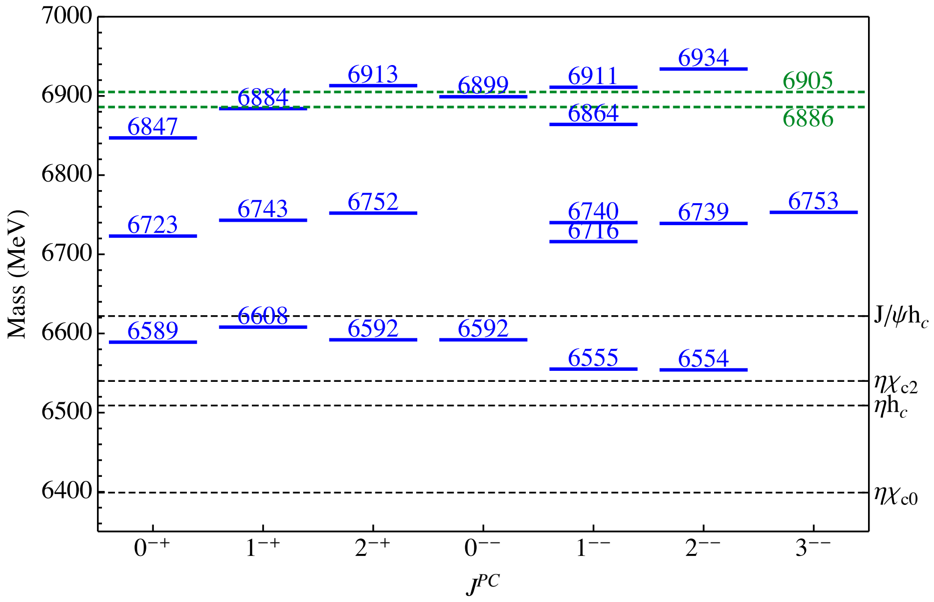

- The $V_{so}^{(1)} + V_{tens}^{(1)}$ contributes to the mass shifts and small mixing of λ- and ρ-mode excitations.
- $T_{cc\bar{c}\bar{c}}$ is domananted by one excitation mode.
- The lowest P-wave $T_{cc\bar{c}\bar{c}}$'s are almost be ρ-mode excitation with $6_c - \bar{6}_c$ configurations.
- $X(6900)$: Narrow P-wave state : $J^{PC} = 1^{-+}$ or 2^{-+}.

P-wave $T_{cc\bar{c}\bar{c}}$

- With $V_{so}^{(1)} + V_{tens}^{(1)}$

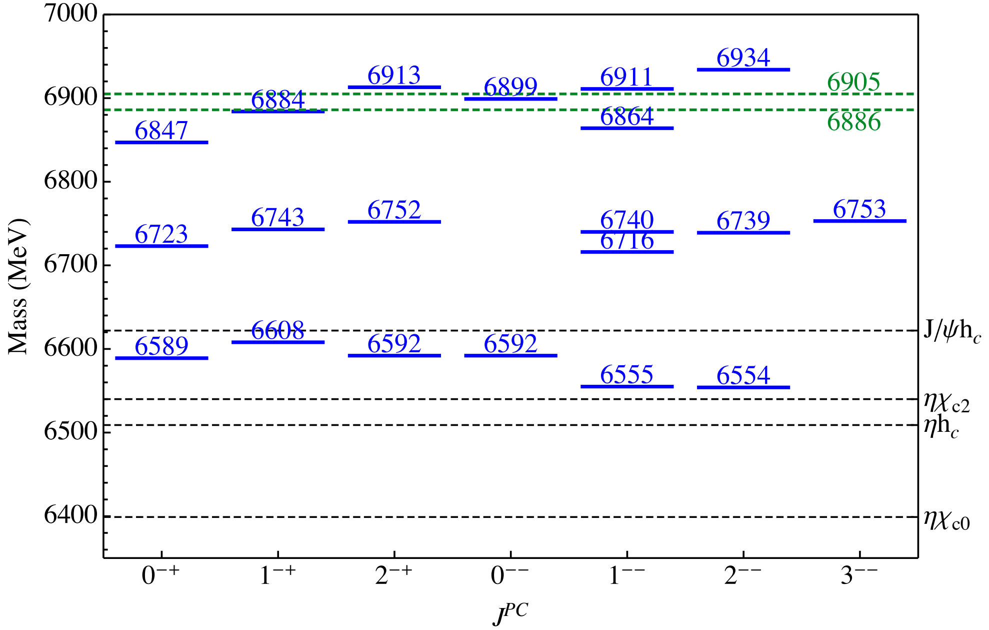

J^{PC}	Decay Modes
0^{-+}	$\boldsymbol{J/\psi J/\psi}$(P-wave), $\eta_c\chi_{c0}$, $J/\psi h_c$, $J/\psi\psi(2S)$(P-wave)
1^{-+}	$\boldsymbol{J/\psi J/\psi}$(P-wave) $J/\psi h_c$, $J/\psi\psi(2S)$(P-wave)
2^{-+}	$\boldsymbol{J/\psi J/\psi}$(P-wave), $\eta_c\chi_{c2}$, $J/\psi h_c$, $J/\psi\psi(2S)$(P-wave)
0^{--}	$\eta_c J/\psi$(P-wave), $J/\psi\chi_{c1}$, $\eta_c\psi(2S)$(P-wave)
1^{--}	$\eta_c J/\psi$(P-wave), $\eta_c h_c$, $J/\psi\chi_{c0}$, $J/\psi\chi_{c1}$, $J/\psi\chi_{c2}$, $\eta_c\psi'$(P-wave)
2^{--}	$\eta_c J/\psi$(P-wave), $J/\psi\chi_{c1}$, $J/\psi\chi_{c2}$, $\eta_c\psi'$(P-wave), $h_c\chi_{c0}$(P-wave)
3^{--}	$J/\psi\chi_{c2}$

- The phase-space-allowed decay modes for the lowest P-wave $T_{cc\bar{c}\bar{c}}$'s are the P-wave channels.
- The P-wave $T_{cc\bar{c}\bar{c}}$'s are narrow.
- $X(6900)$: Narrow P-wave state $J^{PC} = 1^{-+}$ or 2^{-+}.

Discussion

- For a confined charmonium $\bar{c}c$, the H in harmonic oscillator potential is

$$H = \sum_i \frac{p_i^2}{2m_i} + kr_{12}^2 = \frac{p^2}{2u_m} + \frac{u_m\omega^2}{2} r_{12}^2, \quad \text{with} \quad u_m = \frac{m_Q}{2}, \quad \omega_m = \sqrt{\frac{4k}{m_Q}},$$

- $\bar{c}c$: $m_P - m_S = \hbar\sqrt{\frac{4k}{m_Q}} \approx 400 \sim 500$ MeV.

- For a confined $T_{cc\bar{c}\bar{c}}$,

$$H = \sum_{i=1}^{4} \frac{\mathbf{p}_i^2}{2m_i} + a_1 k(r_{12}^2 + r_{34}^2) + a_2 k'(r_{13}^2 + r_{24}^2 + r_{14}^2 + r_{23}^2)$$
$$= \frac{\mathbf{p}_a^2}{2u_a} + \frac{\mathbf{p}_b^2}{2u_b} + \frac{\mathbf{p}_{ab}^2}{2u_{ab}} + \frac{u_a\omega_\rho^2}{2} r_{12}^2 + \frac{u_b\omega_\rho^2}{2} r_{34}^2 + \frac{u_{ab}\omega_\lambda^2}{2} r^2,$$

	a_1	a_2	ω_ρ	ω_λ
$\bar{3}_c - 3_c$	$\frac{1}{2}$	$\frac{1}{4}$	$\sqrt{\frac{2k+k'}{2u_a}}$	$\sqrt{\frac{-2k+5k'}{4u_a}}$
$6_c - \bar{6}_c$	$-\frac{1}{4}$	$\frac{5}{8}$	$\sqrt{\frac{2k'}{u_{ab}}}$	$\sqrt{\frac{-2k+5k'}{4u_b}}$

- If $k = k'$, $6_\rho < 3_\lambda < 3_\rho < 6_\lambda$.

- $T_{cc\bar{c}\bar{c}}$: $m_P - m_S = \hbar\omega_\lambda = \hbar\sqrt{\frac{3k}{2m_Q}} \approx 245 \sim 300$ MeV.

Dynamical calculation:

- P-wave $T_{cc\bar{c}\bar{c}}$: $6_\rho < 3_\lambda < 6_\lambda < 3_\rho$

- Small mass gap between S-wave and P-wave $T_{cc\bar{c}\bar{c}}$.

Summary

- S-wave states

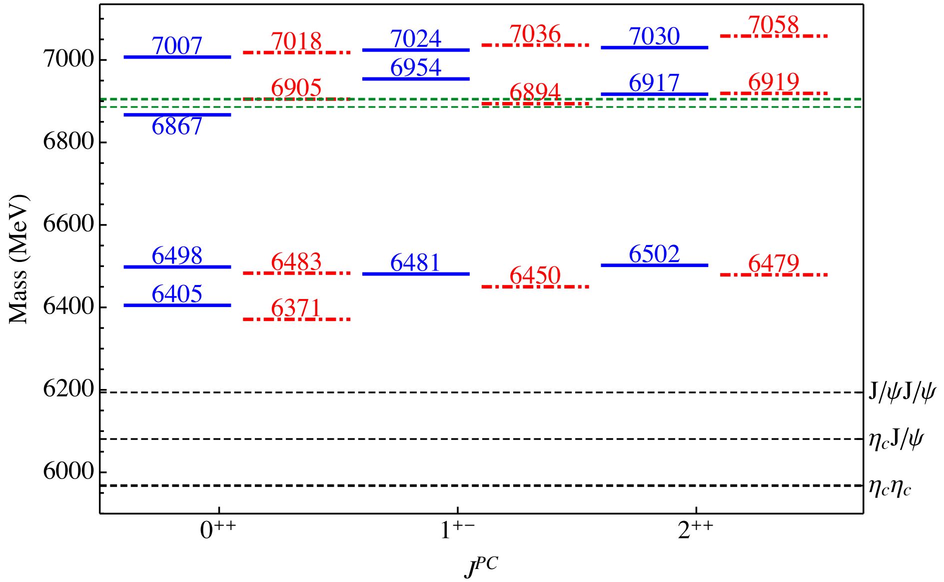

- P-wave states

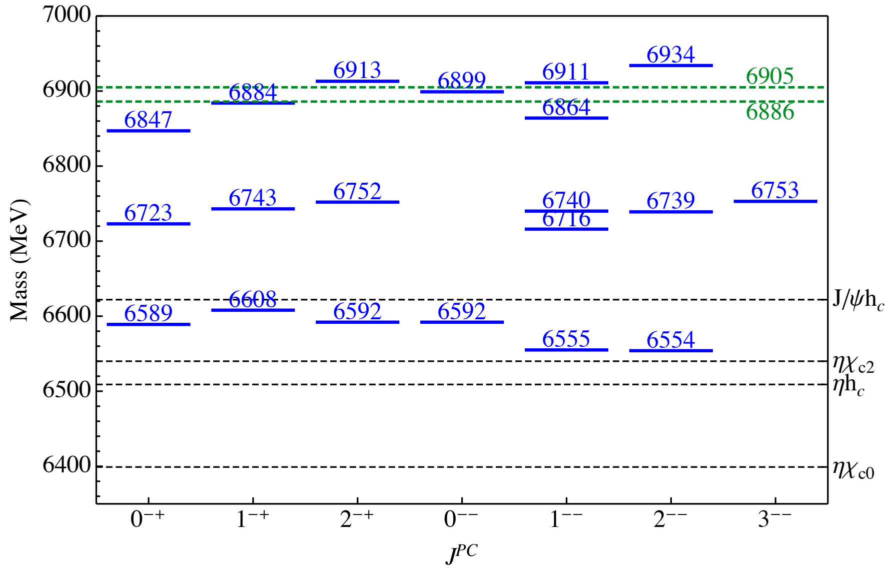

- The mass spectrum of the fully charmed tetraquark state : quark model & Gaussian expansion method.
- $6_c - \bar{6}_c$ is important even dominant in the ground state.
- No stable bound states exist in the quark models.
- $X(6900)$: wide S-wave states $J^{PC} = 0^{++}$ or 2^{++} or Narrow P-wave state : $J^{PC} = 1^{-+}$ or 2^{-+}.

Thank you for your attention!

Back up side

Number of base

- The dependence of the mass spectra on the number of the expanding base.

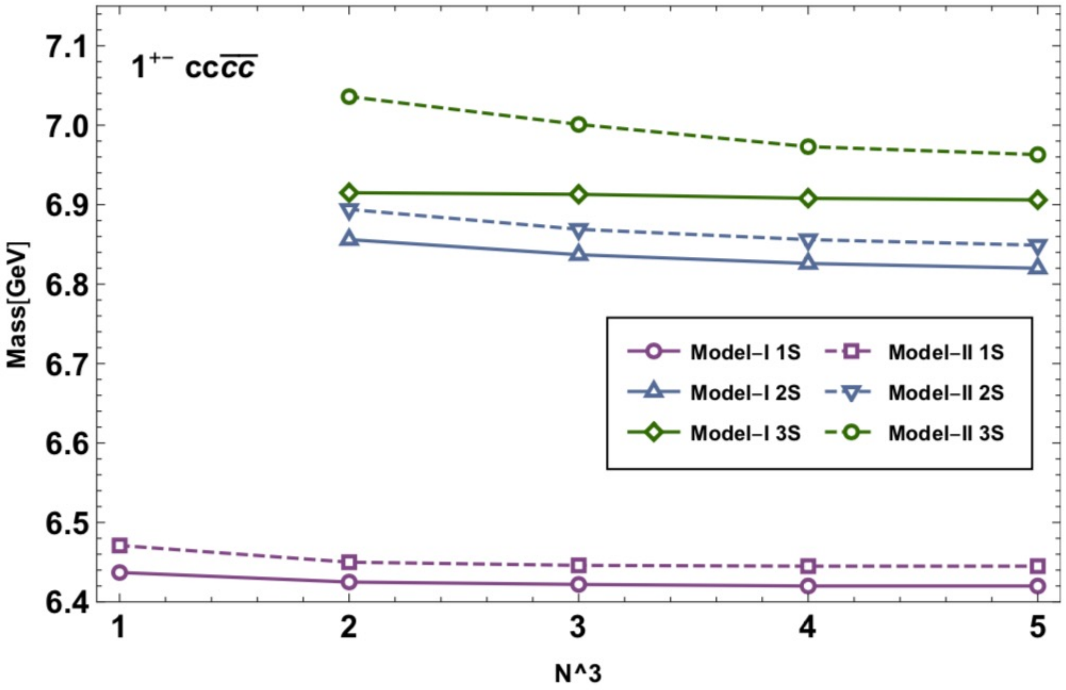

FIG. 2. The dependence of the mass spectrum on the number of Gaussian basis N^3. The line and dashed line represent the numerical results in model I and model II, respectively.

✓ $N^3 = 2^3$

Tetraquark

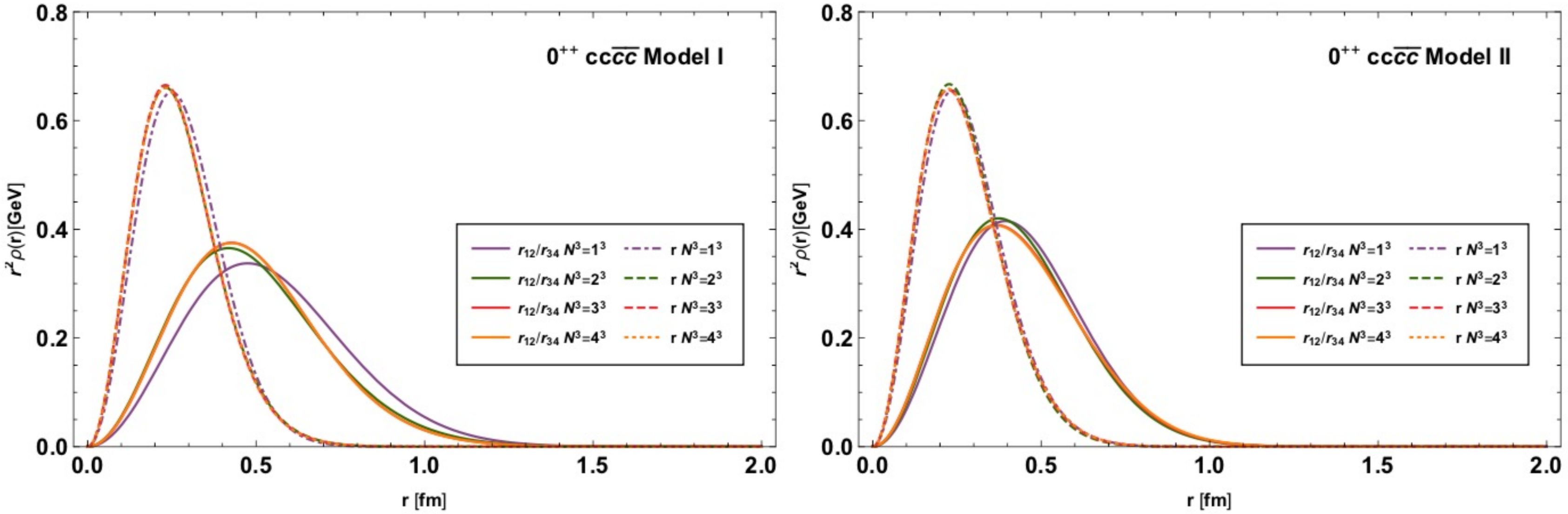

(a) Model I.

(b) Model II.

FIG. 1: The dependence of the root mean square radius $\sqrt{\langle r_{12}\rangle}$ ($\sqrt{\langle r_{34}\rangle}$) and $\sqrt{\langle r\rangle}$ on the extension of the wave function.

$$\rho(r) = \int |\psi(r_{12},\, r_{34},\, r)|^2 d\vec{r}_{12} d\vec{r}_{34} d\hat{\vec{r}}$$

$$\rho(r_{12}) = \int |\psi(r_{12},\, r_{34},\, r)|^2 d\vec{r} d\vec{r}_{34} d\hat{\vec{r}}_{12}$$

S-wave fully-tetraquark state

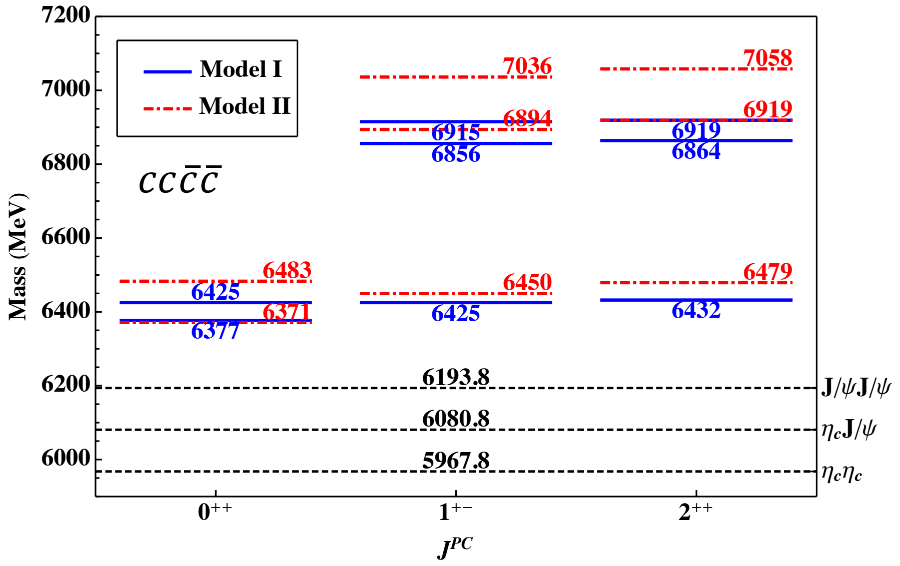

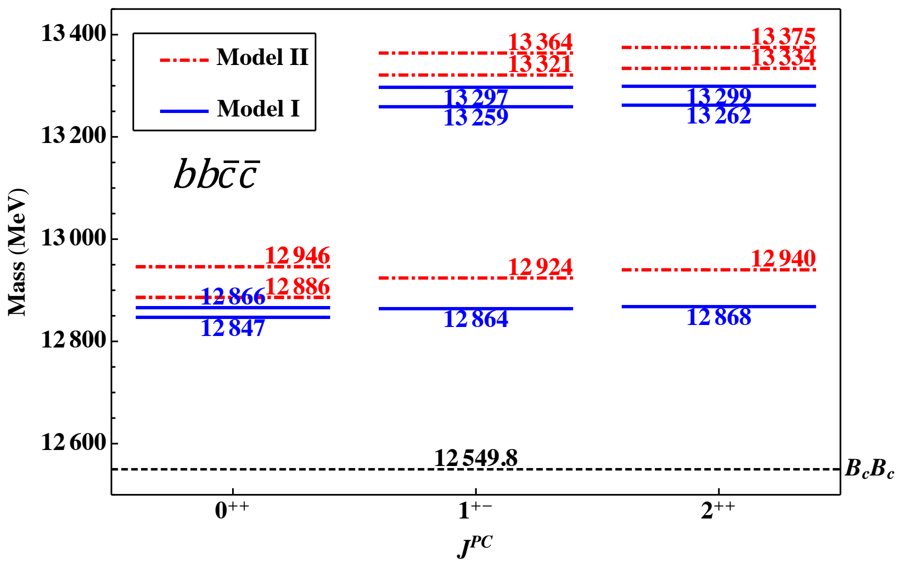

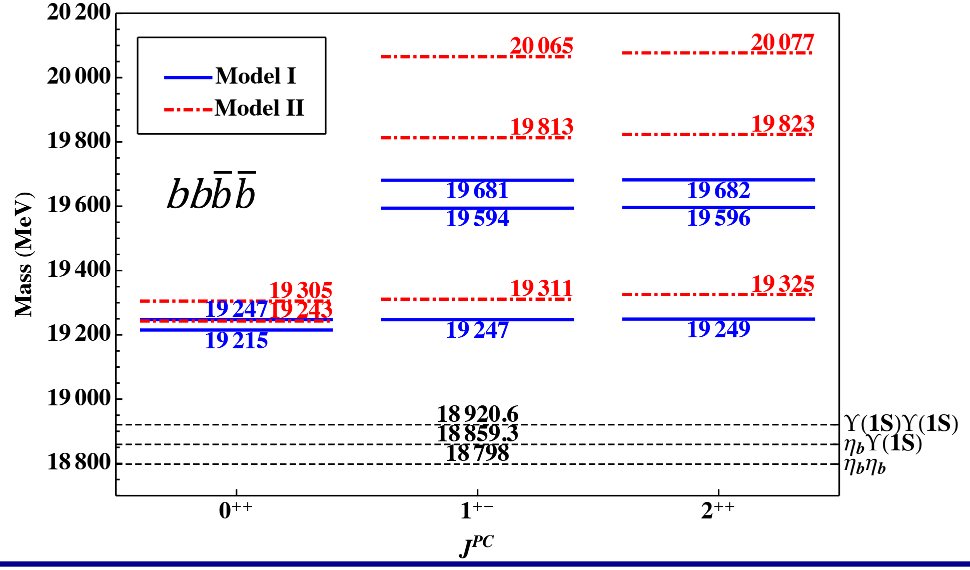

✓ The lowest 0^{++} states are located about 300 ~ 450 MeV above the lowest scattering state.

✓ No bound states exist in the two quark models

Phys. Rev. D. 100, 096013 (2019)

Properties of S-wave state

TABLE IV. The mass spectrum (MeV), the percentage of different color configurations, and the root mean square radius (fm) of the S-wave tetraquark states.

0^{++}	Mass	$\bar{3}_c \otimes 3_c$	$6_c \otimes \bar{6}_c$	$1_c \otimes 1_c$	$8_c \otimes 8_c$	r_{12}/r_{34}	r	r_{13}/r_{24}	r'
1S	6405	31.9%	68.1%	96.9%	3.13%	0.52	0.31	0.48	0.37
	6498	67.7%	32.3%	5.7%	94.3%	0.51	0.36	0.51	0.36
2S	6867	10.6%	89.4%	80.6%	19.4%	0.65	0.35	0.58	0.46
	7007	89.7%	10.3%	26.0%	74.0%	0.49	0.47	0.59	0.35
1^{+-}	Mass	$\bar{3}_c \otimes 3_c$	$6_c \otimes \bar{6}_c$	$1_c \otimes 1_c$	$8_c \otimes 8_c$	r_{12}/r_{34}	r	r_{13}/r_{24}	r'
1S	6481	100%	0%	33.3%	66.7%	0.48	0.37	0.51	0.34
2S	6954	100%	0%	33.3%	66.7%	0.61	0.44	0.61	0.43
3S	7024	100%	0%	33.3%	66.7%	0.66	0.42	0.62	0.46
2^{++}	Mass	$\bar{3}_c \otimes 3_c$	$6_c \otimes \bar{6}_c$	$1_c \otimes 1_c$	$8_c \otimes 8_c$	r_{12}/r_{34}	r	r_{13}/r_{24}	r'
1S	6502	100%	0%	33.3%	66.7%	0.49	0.39	0.53	0.35
2S	6917	100%	0%	33.3%	66.7%	0.55	0.60	0.72	0.39
3S	7030	100%	0%	33.3%	66.7%	0.64	0.46	0.64	0.45

Properties of P-wave state

TABLE VI. The mass spectrum (MeV), the percentages of different λ- and ρ-mode components, and the root mean square radius (fm) of the P-wave tetraquark states. In the second row, we display the mass spectrum obtained with the leading potentials in Eq. (2) and the mass corrections from the perturbative spin-orbital and tensor interactions in the mass matrix.

J^{PC}		Mass	$\vert\lambda_1^{+/-}\rangle$	$\vert\lambda_2^-\rangle$	$\vert\lambda_3^-\rangle$	$\vert\rho_1^{+/-}\rangle$	$\vert\rho_2^{+/-}\rangle$	r_{12}/r_{34}	r	r_{13}/r_{24}	r'
0^{-+}	$\begin{pmatrix} 6746 & 20 & 20 & 34 \\ -20 & 6599+2 & -42 \\ -34 & -42 & 6894-62 \end{pmatrix}$	6589	3.5%			92.8%	3.7%	0.62	0.33	0.60	0.50
		6723	90.4%			5.2%	4.4%	0.52	0.43	0.66	0.37
		6847	6.0%			2.1%	91.9%	0.57	0.38	0.61	0.47
0^{--}	$\begin{pmatrix} 6561+31 & -11 \\ -11 & 6913-14 \end{pmatrix}$	6592				99.9%	0.1%	0.61	0.32	0.59	0.49
		6899				0.1%	99.9%	0.58	0.38	0.61	0.48
1^{-+}	$\begin{pmatrix} 6746-3 & -4 & -6 \\ -4 & 6599+9 & 8 \\ -6 & 8 & 6894-10 \end{pmatrix}$	6608	0.1%			99.8%	0.1%	0.63	0.33	0.60	0.50
		6743	99.7%			0.1%	0.2%	0.51	0.43	0.66	0.36
		6884	0.2%			0.1%	99.7%	0.57	0.37	0.60	0.47
1^{--}	$\begin{pmatrix} 6740 & -2 & 0 & -10 & 9 \\ -2 & 6741-23 & 7 & -19 & 26 \\ 0 & 7 & 6885 & -2 & -25 \\ -10 & -19 & -2 & 6561-1 & 21 \\ 9 & 26 & -25 & 21 & 6913-28 \end{pmatrix}$	6555	0.3%	1.6%	$\sim 0\%$	97.5%	0.6%	0.61	0.32	0.59	0.49
		6716	0.6%	94.8%	0.4%	2.0%	2.1%	0.52	0.42	0.65	0.37
		6740	98.8%	0.9%	$\sim 0\%$	0.2%	0.1%	0.51	0.43	0.65	0.36
		6864	0.2%	2.2%	55.7%	0.1%	41.9%	0.62	0.35	0.64	0.47
		6911	0.1%	0.5%	43.9%	0.2%	55.3%	0.61	0.36	0.63	0.47
2^{-+}	$\begin{pmatrix} 6746+6 & 7 & 10 \\ 7 & 6599-6 & 13 \\ 10 & 13 & 6894+18 \end{pmatrix}$	6592	0.2%			99.7%	0.1%	0.63	0.33	0.60	0.50
		6752	99.4%			0.2%	0.4%	0.52	0.43	0.66	0.36
		6913	0.4%			0.2%	99.4%	0.57	0.38	0.60	0.47
2^{--}	$\begin{pmatrix} 6741-2 & 7 & -9 \\ 7 & 6561-6 & -15 \\ -9 & -15 & 6913+20 \end{pmatrix}$	6554		0.1%		99.7%	0.2%	0.61	0.32	0.59	0.49
		6739		99.6%		0.1%	0.2%	0.51	0.43	0.66	0.36
		6934		0.2%		0.2%	99.6%	0.57	0.38	0.61	0.48
3^{--}	$6741+11$	6753		100%				0.51	0.43	0.66	0.36